Science AAAS

Itokawa Dust Particles: A Direct Link Between S-Type Asteroids and Ordinary Chondrites

Tomoki Nakamura *et al.*

Science **333**, 1113 (2011);
DOI: 10.1126/science.1207758

Itokawa Dust Particles: A Direct Link Between S-Type Asteroids and Ordinary Chondrites

Tomoki Nakamura,[1]* Takaaki Noguchi,[2] Masahiko Tanaka,[3] Michael E. Zolensky,[4] Makoto Kimura,[2] Akira Tsuchiyama,[5] Aiko Nakato,[1] Toshihiro Ogami,[1] Hatsumi Ishida,[1] Masayuki Uesugi,[6] Toru Yada,[6] Kei Shirai,[6] Akio Fujimura,[6] Ryuji Okazaki,[7] Scott A. Sandford,[8] Yukihiro Ishibashi,[6] Masanao Abe,[6] Tatsuaki Okada,[6] Munetaka Ueno,[6] Toshifumi Mukai,[6] Makoto Yoshikawa,[6] Junichiro Kawaguchi[6]

The Hayabusa spacecraft successfully recovered dust particles from the surface of near-Earth asteroid 25143 Itokawa. Synchrotron-radiation x-ray diffraction and transmission and scanning electron microscope analyses indicate that the mineralogy and mineral chemistry of the Itokawa dust particles are identical to those of thermally metamorphosed LL chondrites, consistent with spectroscopic observations made from Earth and by the Hayabusa spacecraft. Our results directly demonstrate that ordinary chondrites, the most abundant meteorites found on Earth, come from S-type asteroids. Mineral chemistry indicates that the majority of regolith surface particles suffered long-term thermal annealing and subsequent impact shock, suggesting that Itokawa is an asteroid made of reassembled pieces of the interior portions of a once larger asteroid.

The Hayabusa spacecraft arrived at S(IV)-type asteroid 25143 Itokawa (formerly 1998 SF36) in September 2005 (*1*). Remote-sensing measurements from the spacecraft suggest that Itokawa consists of rocks similar to LL5 and LL6 ordinary chondrites (*2*, *3*), confirming ground-based spectral characterization (*4*). On 20 and 26 November 2005, the spacecraft descended to touchdown and capture dust particles from MUSES-C Regio. This area consists of dust and gravel deposits dominated by grains up to 1 cm in diameter (*5*). Although the sampler did not operate as planned, an elastic sampling horn impacted onto the asteroid surface, directing dust particles into the spacecraft's sample catcher device (*5*). The Hayabusa sample capsule successfully landed in the Woomera Prohibited Area in South Australia on 13 June 2010. Dust particles collected at the second touchdown were recovered by two methods. In one method, we used a Teflon spatula to sweep particles from about 10% of the surface of a sample catcher. In the other method, we gently tapped on the exterior of the sample catcher, causing particles to drop onto a pure silica glass slide (*6*).

[1]Department of Earth and Planetary Material Sciences, Faculty of Science, Tohoku University, Aoba, Sendai, Miyagi 980-8578, Japan. [2]College of Science, Ibaraki University, 2-1-1 Bunkyo, Mito, Ibaraki 310-8512, Japan. [3]Synchrotron X-ray Station at SPring-8, National Institute for Materials Science, Sayo, Hyogo 679-5198, Japan. [4]ARES, NASA Johnson Space Center, Houston, TX 77058, USA. [5]Department of Earth and Space Science, Graduate School of Science, Osaka University, Toyonaka 560-0043, Japan. [6]JAXA-ISAS, 3-1-1 Yoshinodai, Sagamihara, Kanagawa 229-8510, Japan. [7]Department of Earth and Planetary Science, Faculty of Science, Kyushu University, Hakozaki, Fukuoka 812-8581, Japan. [8]NASA Ames Research Center, Moffett Field, CA 94035, USA.

*To whom correspondence should be addressed. E-mail: tomoki@m.tohoku.ac.jp

On the Teflon spatula, we identified 1534 rocky particles by means of a field-emission scanning electron microscope. The particles have diameters ranging from 3 to 40 μm but are mostly smaller than 10 μm (*7*). Most Itokawa particles are angular and are probably broken pieces of larger rocks. Among the 1534 harvested rocky particles, 1087 are monomineralic, including 580 olivine particles, 126 low-Ca pyroxenes, 56 high-Ca pyroxenes, 186 feldspars (172 plagioclase and 14 K-feldspar), 113 troilites, 13 chromites, 10 Ca phosphates, and 3 Fe-Ni metal grains. The remaining 447 particles are polymineralic mixtures, mainly silicates. Several other particles are silica minerals and K-bearing halite, all of uncertain origin.

Of the 40 particles removed by tapping (diameters ranging from 30 to 180 μm) that were analyzed by x-ray computed microtomography (*7*) and x-ray diffraction, 38 were subjected to more detailed mineralogic analysis. Backscattered electron images of selected particles are shown in Fig. 1, A to D. RA-QD02-0030 (Fig. 1A) and RA-QD02-0024 (Fig. 1B) have a platy morphology, are polymineralic, and have many mineral grains 1 to 10 μm in diameter adhering to their surfaces. Their appearance is typical of most Itokawa particles. Two particles show different morphologies. RA-QD02-0013 (Fig. 1C) has a smoother soccer-ball shape, whereas RA-QD02-0027 (Fig. 1D) consists of a large troilite crystal and smaller silicates. Particles that contain troilite or taenite as major components like RA-QD02-0027 are rare.

Mineralogical analysis of individual "tapped" particles indicates that they consist mainly of coarse [typically 10 to 50 μm in diameter (*7*)] crystalline silicates, the most abundant being olivine. The next most abundant minerals are low- and high-Ca pyroxene and plagioclase (fig. S6A). Low-Ca pyroxene is exclusively composed of orthopyroxene, except for RA-QD02-0060, which is dominated by low-Ca clinopyroxene (monoclinic structure was confirmed by x-ray diffraction). The degree of crystallinity of silicates differs between and within particles, particularly for plagioclase. Some particles contain chromite, chlorapatite, merrillite, and troilite up to 25 μm in size. Small inclusions (up to 10 μm) of taenite, kamacite, troilite, and

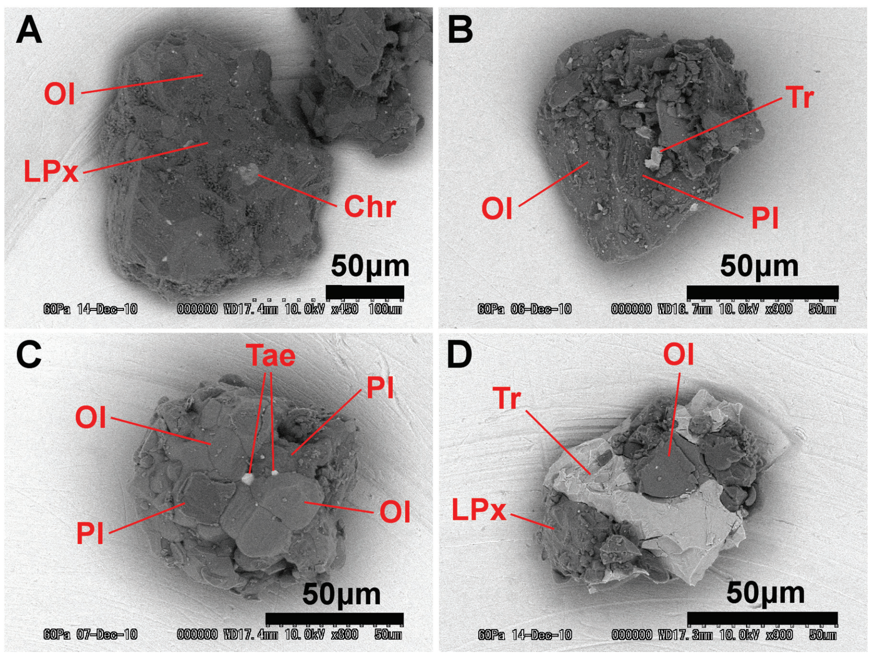

Fig. 1. (**A** to **D**) Backscattered electron (BSE) images of RA-QD02-0030 (A), RA-QD02-0024 (B), RA-QD02-0013 (C), and RA-QD02-0027 (D).

chromite occur within coarse silicates in many particles. The occurrence of triple junctions at the boundary between coarse silicates suggests that most particles have been thermally annealed. Internal, frequently elongate, pores in silicates defining curved planes are interpreted as partially healed, impact-generated fractures (*7*).

Silicates in 38 of the "tapped" Itokawa particles show a limited compositional range. Of these, olivine was found in 29, with an average compositional range of $Fa_{28.6\pm1.1}$ (Fig. 2, A and B). Low-Ca pyroxene (present in 15 particles) is $Fs_{23.1\pm2.2}Wo_{1.8\pm1.7}$ (Fig. 2, A and C); high-Ca pyroxene (present in 14 particles) is $Fs_{8.9\pm1.6}Wo_{43.5\pm4.5}$ (Fig. 2C); and plagioclase (present in 23 particles) is $Ab_{83.9\pm1.3}Or_{5.5\pm1.2}$. FeNi metallic inclusions within silicates show a narrow compositional range: Ni and Co concentrations for kamacite are 3.8 to 4.2 weight percent (wt%) and 9.4 to 9.9 wt%, respectively, and those for taenite are 42 to 52 wt% and 2.0 to 2.5 wt%, respectively. Compositional ranges of olivine, low-Ca pyroxene, and Co and Ni concentrations in kamacite for equilibrated members (petrologic types 4 to 6) of the main ordinary chondrite groups are as follows: H (Fa_{16-20}, $Fs_{14.5-18}$, 0.44 to 0.51 wt% Co, ~6.9 wt% Ni), L (Fa_{22-26}, Fs_{19-22}, 0.70 to 0.95 wt% Co, ~6.54 wt% Ni), and LL (Fa_{26-32}, Fs_{22-26}, 1.42 to 37.0 wt% Co, ~4.98 wt% Ni) (*8*, *9*). Olivine, low-Ca pyroxene, and kamacite compositions of most Itokawa particles fall within the range of LL chondrites, indicating that MUSES-C Regio is covered with LL-chondrite particles.

Close examination of the mineral chemistries of these 38 Itokawa particles revealed that they belong to two different populations: six poorly equilibrated particles and 32 highly equilibrated particles. The poorly equilibrated particles contain olivine and low-Ca pyroxene with compositional ranges $Fa_{24.4-28.9}$ and $Fs_{11.2-23.8}$, respectively (Fig. 2, B and C); pyroxene is more heterogeneous because of slower cation diffusion (*10*). RA-QD02-0060 contains a large low-Ca clinopyroxene crystal with lamellar-like Fe-Mg zoning (Fig. 3A) and Mg-rich host ($Fs_{11.3}Wo_{0.5}$; table S1) with many Mg-poor lamella (~$Fs_{20.4}Wo_{0.6}$; table S1). Three particles contain mesostasis consisting of tiny diopside and troilite crystals embedded in albitic glass (Fig. 3B). The texture and composition of the mesostasis is similar to that of chondrule mesostasis, which suggests that these particles are pieces of chondrules.

The highly equilibrated Itokawa particles (Fig. 1, A to D) have narrow olivine and low-Ca pyroxene compositional ranges of $Fa_{27.1-30.7}$ and $Fs_{22.5-25.7}$, respectively (Fig. 2, B and C). Mesostasis is absent, and coarse-grained diopside and plagioclase (Fig. 3C)—some of which include exsolved K-feldspar (Fig. 3D)—are abundant. Major and minor element concentrations in silicates in these particles are nearly constant within and between particles. The mean compositions of olivine and low- and high-Ca pyroxene are $Fa_{29.0\pm0.7}$, $Fs_{24.0\pm0.6}Wo_{1.4\pm0.3}$, and $Fs_{8.6\pm0.8}Wo_{44.8\pm0.9}$, respectively (table S2). Virtually constant Fs and Wo contents in both low- and high-Ca pyroxenes indicate that the highly equilibrated particles experienced intense thermal metamorphism (*11*); Mg, Fe, and Ca partitioning between pyroxenes has almost progressed to completion.

Ordinary chondrite meteorites exhibit a complete thermal metamorphic sequence from unequilibrated type 3, through types 4 and 5, to totally equilibrated type 6 (*11*). Mg-rich clinopyroxene in type-3 ordinary chondrites is pro-

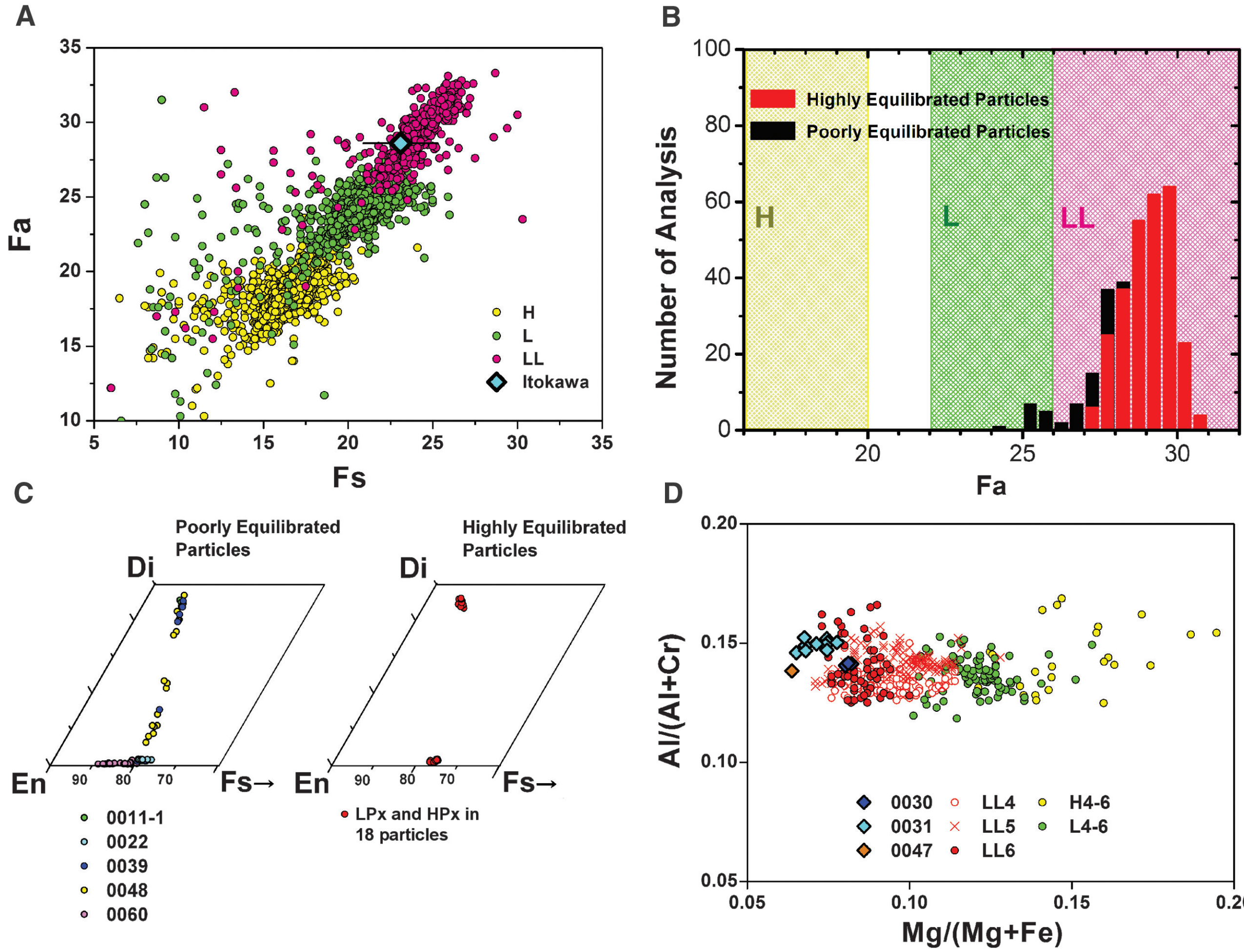

Fig. 2. (**A**) Mean Fa and Fs contents of all tapped Itokawa particles in comparison with those of H, L, and LL chondrites. (**B**) Fa distribution of olivine crystals from 29 Itokawa particles. Approximately 10 analyses were made for each olivine crystal. (**C**) Pyroxene compositions from 5 poorly equilibrated particles (left) and from 18 highly equilibrated particles (right); 5 to 10 analyses were made for each pyroxene crystal. (**D**) Chromite compositions of three highly equilibrated particles: RA-QD02-0030, -0031, and -0047. Chromite data of meteorites are from (*16*).

gressively transformed to orthopyroxene with increasing metamorphism. Devitrified chondrule mesostasis glass (table S1), clinopyroxene, and the characteristic lamellar-like Fe-Mg zoning (like that in the poorly equilibrated Itokawa particles) is present in type 4 ordinary chondrites but absent in type 5 (*12*, *13*). Thus, the poorly equilibrated Itokawa particles are weakly metamorphosed material, classified as petrologic type 4.

The narrow compositional variations of the highly equilibrated Itokawa pyroxenes (Fig. 2C) are similar to LL5 and LL6 chondrites (*10*, *14*). The characteristics of high-temperature metamorphism of grades 5 and 6 (*14*) that we observe in highly equilibrated Itokawa particles include (i) very low CaO and Cr_2O_3 contents (<0.02 wt%) in olivine, (ii) predominance of low-Ca orthopyroxene over clinopyroxene (Fig. 3E), (iii) preferential occurrence of diopside and absence of augite (Fig. 2C), and (iv) presence of coarsened plagioclase (typically 20 to 50 μm in diameter; Fig. 3C) and diopside (typically 10 to 30 μm). Similarly, chromite in the highly equilibrated particles has compositions (Fig. 2D and table S3) similar to those of LL5 and LL6 chondrites (*15*, *16*). Thus, the highly equilibrated particles formed during intense thermal metamorphism. Itokawa is a breccia of poorly equilibrated LL4 and highly equilibrated LL5 and LL6 materials. The conclusion is confirmed by independent results of a companion paper (*7*).

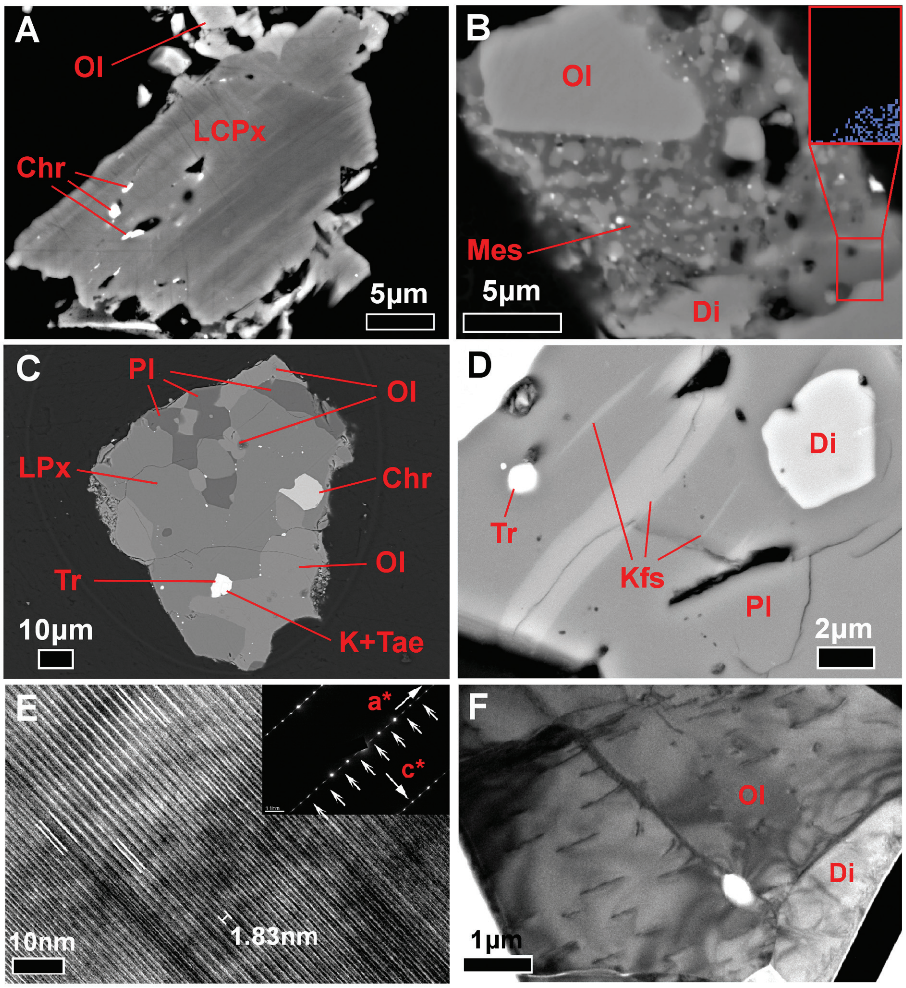

Fig. 3. (**A** to **F**) Poorly equilibrated particles RA-QD02-0060 (A) and RA-QD02-0011-1 (B). Highly equilibrated particles RA-QD02-0030 (C), RA-QD02-0013 (D), RA-QD02-0024 (E), and RA-QD02-0032 (F). (A) Thin, FeO-rich light lamellae repeatedly occur in Low-Ca clinopyroxene. (B) Mesostasis glass-like portions occur between coarse silicate crystals. Inset: An EBSD map (red box) indicates that mesostasis shows no diffraction and thus it is glass. (C) A variety of minerals are included in this particle. (D) Three parallel exsolution lamella of K-feldspar sanidine occur in albite. (E) Low-Ca pyroxene consists of orthopyroxene with many stacking disorders parallel to (100). Inset: Diffraction spots show streaks (indicated by arrows) due to disturbance of the 1.8-nm repetition (indicated by white lines). (F) The dislocation density in this olivine is 1.6×10^8 cm^{-2}, suggestive of moderate shock. (A) to (D), BSE images; (E) and (F), bright-field transmission electron microscope images. Ol, olivine; LPx, low-Ca pyroxene; LCPx, low-Ca clinopyroxene; Di, diopside; Chr, chromite; Tr, troilite; K, kamacite; Tae, taenite; Pl, plagioclase; Kfs, K feldspar; Mes, mesostasis.

With our mineralogic data of the highly equilibrated particles, it is possible to follow three critical phases of Itokawa's thermal evolution. The prograde peak crystallization temperature is provided by plagioclase triclinicity (*6*, *17*, *18*) from five particles: 570°C for RA-QD02-0010, 560°C for RA-QD02-0025-01, 570°C for RA-QD02-0055, 575°C for RA-QD02-0067, and 820°C for RA-QD02-0013. These plagioclases crystallized at different points as temperatures rose to a peak of 820°C, with each crystal locking in a different triclinicity (*18*, *19*). The peak metamorphic temperature (i.e., the temperature of last equilibration) is revealed by two-pyroxene geothermometry (*20*). Low- and high-Ca pyroxenes with homogeneous compositions coexist in three Itokawa particles, and peak metamorphic temperatures at 0.1 MPa were calculated using QUILF 95 software: 783° ± 12°C for RA-QD02-0013, 814° ± 21°C for RA-QD02-0024, and 837° ± 10°C for RA-QD02-0010. These temperatures are slightly lower than the range reported for LL6 chondrite meteorites [875° to 945°C (*19*)]. To characterize the subsequent cooling period, we applied the olivine-spinel geothermometer (*21*) to three particles containing olivine-chromite pairs: RA-QD02-0030 (Figs. 1A and 3C), -0031, and -0047, in which yielded equilibration temperatures of 636°C, 625°C, and 595°C, respectively. These temperatures are lower than those obtained by two-pyroxene thermometry, reflecting continued Fe-Mg exchange between chromite and olivine during cooling, which occurred more quickly than Ca diffusion in pyroxene (*10*). The olivine-spinel geospeedometry (*22*) applied to mean chromite size (~20 μm) and the equilibrated temperatures and the results indicate slow cooling at a rate of ~0.5 K per 1000 years near 600°C. The combined results of these temperature estimates suggest that the highly equilibrated particles experienced a peak metamorphic temperature of ~800°C and cooled slowly to 600°C.

During thermal metamorphism in asteroids, temperatures increase with depth and thus higher petrologic-type materials form deeper than the lower types, assuming internal heating due to decay of short-lived radioisotopes such as ^{26}Al (*23*–*25*). The slow cooling of the highly equilibrated Itokawa particles suggests that they formed at considerable depth. The temperature of 800°C experienced by many Itokawa particles requires a diameter of the original asteroid larger than 20 km (*25*). The current size of Itokawa (0.5 × 0.3 × 0.2 km) (*1*) is much smaller than this required size. Therefore, the Itokawa parent S-class asteroid was originally much larger, experienced intense thermal metamorphism, and was then catastrophically disaggregated by one or more impacts into many small pieces, some of which reaccreted into the present greatly diminished, rubble-pile asteroid, consistent with previous suggestions (*1*). Impact processes are responsible for cracks in crystals (*7*), dislocations in some olivine crystals (Fig. 3F), and local variations in the degree of silicate crystallinity. These impact effects vary greatly between particles (fig. S7), which is typical of moderately shocked astromaterial corresponding shock stages up to S4 (*6*, *26*).

MUSES-C Regio probably formed by segregation and accumulation of fine gravel into areas close to the gravitational center of Itokawa due to global-scale electrostatic grain levitation, vibration-induced granular migration, and deposition of slow moving ejecta launched from surface impacts (*27*–*29*). Therefore, particles in MUSES-C Regio originally derived from diverse regions of Itokawa. Fortunately, despite the small mass of the recovered Itokawa samples, they record the critical steps in the history of this asteroid. Itokawa was classified as an S-type asteroid from terrestrial remote sensing, and it has been commonly suggested that S-type asteroids, the most abundant asteroids in the inner asteroid belt, are the parent bodies of ordinary chondrites. Our petrologic data from MUSES-C Regio confirm that Itokawa is indeed an ordinary chondrite (LL4 to LL6), thereby finally linking these asteroids and meteorites.

References and Notes

1. A. Fujiwara *et al.*, *Science* **312**, 1330 (2006).
2. M. Abe *et al.*, *Science* **312**, 1334 (2006).
3. T. Okada *et al.*, *Science* **312**, 1338 (2006).
4. R. Binzel, A. S. Rivkin, S. J. Bus, J. M. Sunshine, T. H. Burbine, *Meteorit. Planet. Sci.* **36**, 1167 (2001).
5. H. Yano *et al.*, *Science* **312**, 1350 (2006).
6. See supporting material on *Science* Online.
7. A. Tsuchiyama *et al.*, *Science* **333**, 1125 (2011).
8. A. J. Brearley, R. H. Jones, *Rev. Mineral.* **36**, 3-1 (1998).
9. A. E. Rubin, *Geochim. Cosmochim. Acta* **54**, 1217 (1990).
10. J. B. Brady, D. J. Cherniak, In *Diffusion in Minerals and Melts*, Y. Zhang, D. J. Cherniak, Eds. (Mineralogical Society of America, Chantilly, VA, 2010), pp. 899–920.
11. W. R. Van Schmus, J. A. Wood, *Geochim. Cosmochim. Acta* **31**, 747 (1967).
12. E. A. Jobbins *et al.*, *Mineral. Mag.* **35**, 881 (1966).
13. T. J. McCoy, E. R. D. Scott, R. H. Jones, K. Keil, G. J. Taylor, *Geochim. Cosmochim. Acta* **55**, 601 (1991).
14. G. R. Huss, A. E. Rubin, J. N. Grossman, in *Meteorites and the Early Solar System II*, D. S. Lauretta, H. Y. McSween Jr., Eds. (University of Arizona Press, Tucson, AZ, 2006), pp. 567–586.
15. T. E. Bunch, K. Keil, K. G. Snetsinger, *Geochim. Cosmochim. Acta* **31**, 1569 (1967).
16. M. Kimura, H. Nakajima, H. Hiyagon, M. K. Weisberg, *Geochim. Cosmochim. Acta* **70**, 5634 (2006).
17. J. V. Smith, *J. Geol.* **80**, 505 (1972).
18. Y. Nakamuta, Y. Motomura, *Meteorit. Planet. Sci.* **34**, 763 (1999).
19. V. Slater-Reynolds, H. Y. McSween Jr., *Meteorit. Planet. Sci.* **40**, 745 (2005).
20. D. H. Lindsley, *Am. Mineral.* **68**, 477 (1983).
21. J. Fabriés, *Contrib. Mineral. Petrol.* **69**, 329 (1979).
22. K. Ozawa, *Geochim. Cosmochim. Acta* **48**, 2597 (1984).
23. M. Miyamoto, N. Fujii, H. Takeda, *Proc. Lunar Planet. Sci.* **12B**, 1145 (1981).
24. M. Trieloff *et al.*, *Nature* **422**, 502 (2003).
25. H. Y. McSween *et al.*, in *Asteroids III*, W. Bottke *et al.*, Eds. (Univ. of Arizona Press, Tucson, AZ, 2002), pp. 559–571.
26. D. Stöffler, K. Keil, E. R. D. Scott, *Geochim. Cosmochim. Acta* **55**, 3845 (1991).
27. H. Miyamoto *et al.*, *Science* **316**, 1011 (2007).
28. P. Lee, *Icarus* **124**, 181 (1996).
29. D. G. Korycansky, E. Asphaug, *Icarus* **171**, 110 (2004).

Acknowledgments: We thank the Hayabusa project team for sample return; KEK for synchrotron experiments; H. Nakano, Y. Yamazaki, K. Shimada, Y. Kakazu, T. Hashimoto, M. Konno, Y. Katsuya, and Y. Matsushita, for technical support; and J. Grossman, T. Ikeda, T. Hokada, K. Ozawa, Y. Nakamuta, and S. Wakita for helpful discussions. Supported by NASA grant 769583.07.03 (M.E.Z. and S.A.S.).

Supporting Online Material
www.sciencemag.org/cgi/content/full/333/6046/1113/DC1
Figs. S1 to S8
Tables S1 to S5
References (*30*–*40*)

2 May 2011; accepted 2 August 2011
10.1126/science.1207758

Oxygen Isotopic Compositions of Asteroidal Materials Returned from Itokawa by the Hayabusa Mission

Hisayoshi Yurimoto,[1]* Ken-ichi Abe,[1] Masanao Abe,[2] Mitsuru Ebihara,[3] Akio Fujimura,[2] Minako Hashiguchi,[1] Ko Hashizume,[4] Trevor R. Ireland,[5] Shoichi Itoh,[1] Juri Katayama,[1] Chizu Kato,[1] Junichiro Kawaguchi,[2] Noriyuki Kawasaki,[1] Fumio Kitajima,[6] Sachio Kobayashi,[1] Tatsuji Meike,[1] Toshifumi Mukai,[2] Keisuke Nagao,[7] Tomoki Nakamura,[8] Hiroshi Naraoka,[6] Takaaki Noguchi,[9] Ryuji Okazaki,[6] Changkun Park,[1] Naoya Sakamoto,[1] Yusuke Seto,[10] Masashi Takei,[1] Akira Tsuchiyama,[4] Masayuki Uesugi,[2] Shigeyuki Wakaki,[1] Toru Yada,[2] Kosuke Yamamoto,[1] Makoto Yoshikawa,[2] Michael E. Zolensky[11]

Meteorite studies suggest that each solar system object has a unique oxygen isotopic composition. Chondrites, the most primitive of meteorites, have been believed to be derived from asteroids, but oxygen isotopic compositions of asteroids themselves have not been established. We measured, using secondary ion mass spectrometry, oxygen isotopic compositions of rock particles from asteroid 25143 Itokawa returned by the Hayabusa spacecraft. Compositions of the particles are depleted in ^{16}O relative to terrestrial materials and indicate that Itokawa, an S-type asteroid, is one of the sources of the LL or L group of equilibrated ordinary chondrites. This is a direct oxygen-isotope link between chondrites and their parent asteroid.

Mineral compositions of asteroids are inferred from visible and near-infrared reflectance spectroscopy. The spectroscopic similarity between some asteroids and meteorites suggests that meteorites come from asteroids and allows indirect assessments of asteroid-meteorite connections and inferences regarding chemical compositions of asteroids (*1*). Of the ~40,000 meteorites we know of, only 14 have had their pre-impact orbits ascertained (*2*). The aphelia of these 14 orbits are located within the Main Asteroid Belt between Martian and Jovian orbits, which is consistent with an asteroidal origin. However, even the parent asteroids of these 14 meteorites have not been identified.

The taxonomy of meteorites largely has been based on the whole-rock chemical and oxygen isotopic compositions. Each meteorite group, and probably each planet, has a characteristic chemical composition and a unique oxygen isotopic composition (*3*, *4*). The origin of oxygen isotopic variations in the solar system is thought to be an isotope-selective photodissociation of carbon monoxide that occurred before planet formation (*5*–*7*). The unique oxygen isotopic composition of a planet is thought to be produced by a combination of gas-dust chemistry and accretion physics in the solar nebula (*6*, *8*). The Earth and the Moon—the only bodies for which we have measurements—have similar oxygen isotopic compositions within an uncertainty of ±0.016 per mil (‰) [2 SD (2σ)] (*9*, *10*). The determination of an oxygen isotopic composition of an asteroid or a planet therefore would provide an indisputable means to clarify mechanisms of planet formation in the solar nebula and to connect an asteroid or a planet to a specific meteorite group.

The Hayabusa spacecraft made two touchdowns on the surface of asteroid 25143 Itokawa on 20 and 26 November 2005 JST and successfully collected grain particles from the surface of the asteroid. Itokawa is classified as an S-type asteroid. As inferred from reflectance spectrometry, it consists of materials similar to primitive

[1]Natural History Sciences, Hokkaido University, Sapporo 060-0810, Japan. [2]Japan Aerospace Exploration Agency–Institute of Space and Astronautical Science, 3-1-1 Yoshinodai, Chuo Sagamihara, Kanagawa, 252-5210, Japan. [3]Graduate School of Science and Engineering, Tokyo Metropolitan University, 1-1 Minami-Osawa, Hachioji, Tokyo 192-0397, Japan. [4]Department of Earth and Space Science, Osaka University, 1-1 Machikaneyama, Toyonaka 560-0043, Osaka, Japan. [5]Research School of Earth Sciences, College of Physical and Mathematical Sciences, Australian National University, Canberra, ACT 0200, Australia. [6]Department of Earth and Planetary Sciences, Kyushu University, 6-10-1 Hakozaki, Higashi-ku, Fukuoka 812-8581, Japan. [7]Geochemical Research Center, University of Tokyo, Hongo, Tokyo 113-0033, Japan. [8]Department of Earth and Planetary Material Sciences, Tohoku University, Aramaki, Aoba, Sendai, Miyagi 980-8578, Japan. [9]Collage of Science, Ibaraki University, 2-1-1 Bunkyo, Mito, Ibaraki 310-8512, Japan. [10]Department of Earth and Planetary Sciences, Kobe University, Kobe 657-8501, Japan. [11]Astromaterials Research and Exploration Science, KT, NASA Johnson Space Center, Houston, TX 77058, USA.

*To whom correspondence should be addressed. E-mail: yuri@ep.sci.hokudai.ac.jp